Template Synthesis of a Tetraazamacrocyclic Ligand with Two Pendant Pyridinyl Groups: Properties of the Isomers of the Metal-Free Ligand and of Their First-Row Transition Metal Compounds

Peter Comba,* Stephan M. Luther, Oliver Maas, Hans Pritzkow, and Annette Vielfort

Universitat Heidelberg, Anorganisch-Chemisches Institut, Im Neuenheimer Feld 270, D-69120 Heidelberg, Germany

Received June 27, 2000

The one-step reaction of $[Cu(en)_2]^{2+}$ (en = 1,2-diaminoethane) with formaldehyde, ethyl 2-pyridyl acetate, and base produces a mixture of $[Cu(s\text{-}pypymac)]^{2+}$ and $[Cu(a\text{-}pypymac)]^{2+}$ (s-pypymac = *syn*-6,13-bis(2-pyridinyl)-1,4,8,11-tetraazacyclotetradecane, a-pypymac = *anti*-6,13-bis(2-pyridinyl)-1,4,8,11-tetraazacyclotetradecane; syn-to-anti ratio approximately 1:9) in low yield (6%). Ion exchange chromatography is used for isomer separation, and the two isomers of the metal-free ligand are obtained by reduction of the copper(II) complexes and subsequent ion exchange chromatography. Crystal structure analyses of the metal-free a-pypymac ligand, of two isomeric copper(II) compounds of a-pypymac and one of s-pypymac, and of the cobalt(III) complexes of a- and s-pypymac and nickel(II), as well as zinc(II) complexes of a-pypymac, are reported and discussed on the basis of the expectations from force field calculations and from published experimental data of the transition metal compounds of the bis-pendant amine derivative diammac.

Introduction

The transition metal coordination chemistry of macrocyclic ligands has been developed extensively in the past decades.[1−6] For various applications tetraazamacrocyclic ligands are of special interest, and coordinating side chains may increase the stability of the metal complexes and tune the selectivity between various metal ions.[7,8] Pendant groups are also used to attach substrates covalently, to enforce specific oxidation states and coordination geometries, and to influence the strength of the ligand field.[7,8] Template reactions have been used extensively for the easy, high-yielding and stereospecific synthesis of complex ligand molecules.[6,9−16] Following the successful synthesis of the sepulchrate- and sarcophagine-type hexaamine cage molecules[14−16] the metal ion-directed Mannich condensation of coordinated primary amines with formaldehyde and carbon acids or amines has been used extensively in this field. For macrocyclic and open-chained ligands copper(II) has often been the templating metal ion, but there are also examples of nickel(II)-, palladium(II)-, and gold(III)-directed syntheses.[17−21] Only few aldehydes other than formaldehyde have been employed,[22−24] but a range of acidic "locking groups" lead to interesting geometries of the caping groups[19,25−28] and to electrochemically active,[29] charged (specific electrostatic interactions),[30] or in terms of hydrogen bonding (supramolecular interactions)[31,32] active pendant groups. Open-chained tetradentate,[33−36] macrocyclic,[7] and bis- and tris-macrocyclic ligands have been isolated and

* Corresponding author. Fax: +49(6221)-54-6617. E-mail: comba@akcomba.oci.uni-heidelberg.de.

(1) Melson, G. A. E. *Coordination Chemistry of Macrocyclic Complexes*; Plenum Press: New York, 1982.
(2) Lindoy, L. F. *The chemistry of macrocyclic ligand complexes*; Cambridge University Press: Cambridge, New York, 1989.
(3) Dietrich, B.; Viout, P.; Lehn, J.-M. *Macrocyclic chemistry. Aspects of organic, inorganic and supramolecular chemistry*; VCH: New York, Weinheim, 1991.
(4) Cox, B. G.; Schneider, H. *Coordination and transport properties of macrocyclic compounds in solution*; Elsevier: Amsterdam, London, 1992; Vol. 76.
(5) Cooper, S. R. *Crown compounds: Toward Future Applications*; VCH: Weinheim, New York, 1992.
(6) Gerbeleu, N. V.; Arion, V. B.; Burgess, J. *Template Synthesis of Macrocyclic Compounds*; Wiley-VCH: Weinheim, New York, 1999.
(7) Bernhardt, P. V.; Lawrance, G. A. *Coord. Chem. Rev.* **1990**, *104*, 297.
(8) Kaden, T. A. In *Crown Compounds—Towards Future Applications*; Cooper, S. R., Ed.; Wiley-VCH: Weinheim, New York, 1992.
(9) Comba, P.; Curtis, N. F.; Lawrance, G. A.; Sargeson, A. M.; Skelton, B. W.; White, A. H. *Inorg. Chem.* **1986**, *25*, 4260.
(10) Curtis, N. F. *Coord. Chem. Rev.* **1968**, *3*, 3.
(11) Lindoy, L. F.; Busch, D. H. *Prepr. Inorg. React.* **1971**, *6*, 1.
(12) Thompson, M. C.; Busch, D. H. *J. Am. Chem. Soc.* **1964**, *86*, 213.
(13) Thompson, M. C.; Busch, D. H. *J. Am. Chem. Soc.* **1962**, *84*, 1762.
(14) Sargeson, A. M. *Pure Appl. Chem.* **1984**, *56*, 1603.
(15) Sargeson, A. M. *Coord. Chem. Rev.* **1996**, *151*, 89.
(16) Sargeson, A. M. *Pure Appl. Chem.* **1986**, *58*, 1511.
(17) Curtis, N. F.; Gainsford, G. J.; Hambley, T. W.; Lawrance, G. A.; Morgan, K. R.; Siriwardena, A. *J. Chem. Soc., Chem. Commun.* **1987**, 295.
(18) Kang, S.-G.; Ryu, K.; Suh, M. P.; Jeong, J. H. *Inorg. Chem.* **1997**, *36*, 2478.
(19) Suh, M. P.; Shin, W.; Kim, H.; Koo, C. H. *Inorg. Chem.* **1987**, *26*, 1846.
(20) Rossignoli, M.; Allen, C. C.; Hambley, T. W.; Lawrance, G. A.; Maeder, M. *Inorg. Chem.* **1996**, *35*, 4961.
(21) Rossignoli, M.; Bernhardt, P. V.; Lawrance, G. A.; Maeder, M. *J. Chem. Soc., Dalton Trans.* **1997**, 323.
(22) Bernhardt, P. V.; Byriel, K. A.; Kennard, C. H. L.; Sharpe, P. C. *J. Chem. Soc., Dalton Trans.* **1996**, 145.
(23) Fabbrizzi; L.; Licchelli, M.; Lanfredi, A. M. M.; Vassalli, O.; Ugozzoli, F. *Inorg. Chem.* **1996**, *35*, 1582.
(24) Bernhardt, P. V.; Sharpe, P. C. *Inorg. Chem.* **1998**, *37*, 1629.
(25) Lampeka, Y. D.; Prikhod'ko, A. I.; Nazarenko, A. Y.; Rusanov, E. B. *J. Chem. Soc., Dalton Trans.* **1996**, 2017.
(26) Suh, M. P.; Kang, S.-G.; Goedken, V. L.; Park, S.-H. *Inorg. Chem.* **1991**, *30*, 365.
(27) Comba, P.; Hilfenhaus, P. *J. Chem. Soc., Dalton Trans.* **1995**, 3269.
(28) Comba, P.; Hilfenhaus, P.; Nuber, B. *Helv. Chim. Acta* **1997**, *80*, 1831.
(29) DeBlas, A.; DeSantis, G.; Fabbrizzi, L.; Licchelli, M.; Mangano, C.; Pallavicini, P. *Inorg. Chim. Acta* **1992**, *202*, 115.
(30) Villanueva, N. D.; Chiang, M. Y.; Bocarsly, J. R. *Inorg. Chem.* **1998**, *37*, 685.
(31) Bernhardt, P. V.; Hayes, E. J. *Inorg. Chem.* **1998**, *37*, 4214.
(32) Bernhardt, P. V.; Lathe, A. J. *Inorg. Chem.* **1999**, *38*, 3481.

10.1021/ic000696x CCC: $20.00
Published on Web 04/06/2001

Chart 1

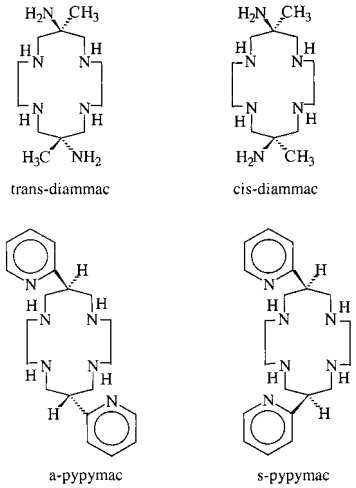

characterized.[27,37,38] The copper(II)-induced reaction, using formaldehyde and nitroethane, has been of particular interest since Zn/HCl reduction leads to the corresponding metal-free ligands with pendant amine donors.[34−36,39]

One of the first and most extensively studied ligands of this type is based on $[Cu(en)_2]^{2+}$, formaldehyde and nitroethane (en = 1,2-diaminoethane; Zn/HCl reduction of the pendant nitro groups to amines), diammac (diammac = 6,13-diamino-6,13-dimethyl-1,4,8,11-tetraazatetradecane, Chart 1). While *trans*-diammac enforces short metal−donor bonds, high ligand fields, and low (negative) reduction potentials,[40−44] *cis*-diammac has a slight preference for trigonal prismatic coordination geometry.[39,45] Complexes of both isomers exist in three possible conformations, and their relative stability depends on the size of the metal ion.[46]

We present here the template synthesis of the diammac derivative pypymac (pypymac = 6,13-bis(2-pyridinyl)-1,4,8,-11-tetraazacyclotetradecane; see Chart 1) together with a structural study of the metal-free ligands and their copper(II), cobalt(III), nickel(II), and zinc(II) complexes.

Results and Discussion

Syntheses. The mechanism of the copper(II)-directed coupling of cis-disposed primary amines has been studied in some detail. The factors relevant to the present study are the following: (i) Condensation of deprotonated, coordinated, primary amines with an aldehyde leads to comparably unstable coordinated imine intermediates; substituted aldehydes (e.g., acetaldehyde, benzaldehyde vs formaldehyde) lead to a stabilization of the imine.[22−24] (ii) Cyclization occurs with a deprotonated "locking group" (C−H-acidic fragment or amine), and the efficiency of the reaction correlates with the acidity of the substrate (nitroethane > sulfonamide > carboxamide > amine > diethylmalonate).[47] (iii) Depending on the workup procedure ester-substituted products may yield the corresponding saponification and decarboxylation products.[48−50] (iv) The fact that the ratio of the two ligand isomers (syn or anti configuration; see Chart 1) depends on the reaction conditions (aqueous or rigorously nonaqueous solutions) and the donor strength of the pendant group suggests that the stereospecificity is due to an axial interaction of the copper(II) center with the substituent of the "locking group".[36,51]

Chart 2

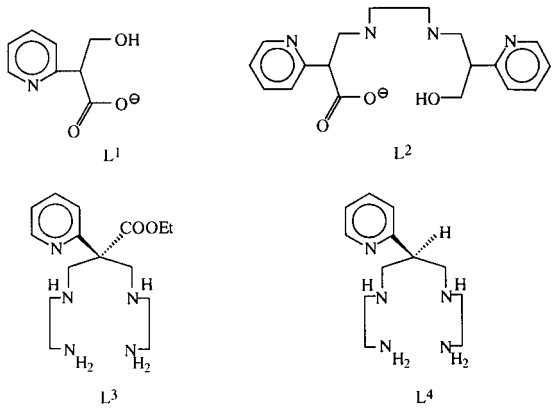

The reaction of $[Cu(en)_2]^{2+}$ with formaldehyde, triethylamine, and ethyl 2-pyridyl acetate yields only traces of the desired product (<1% of $[Cu(s\text{-}/a\text{-}pypymac)]^{2+}$). The major products ($[Cu(L^1)_2]$, $[Cu(L^2)]^+$, $[Cu(L^3)]^{2+}$, Chart 2; see Supporting Information for the crystallographic characterization of some of these side products) suggest that the imine intermediates are rather unstable and/or the saponification/decarboxylation of the ester fragments lead to a deactivation of the C−H-acidic "locking group". Consequently, the yield was increased by reaction in nonaqueous solution (supression of the hydrolysis of the imine) and with DBU (1,8-diazabicyclo[5.4.0]-undec-7-en) as base (reduction of the nucleophilicity due to steric crowding), yielding a purple precipitate, the macrocyclic product coordinated to copper(II). Recrystallization from ethanol/0.1 M perchloric acid (crystallization of the perchlorate salt, decomposition of complexes with acyclic side products) produces 6% of the pure product as an isomeric mixture.

Zn/HCl reduction, followed by chromatographic purification (Dowex 50Wx2), yields a mixture of the isomers of the hydrochlorides of the two metal-free ligands a-pypymac and s-pypymac in a 9:1 ratio (^{1}H NMR; 60−70% overall yield). Ion exchange chromatography of the isomeric mixture of the copper(II) compounds (Dowex 50Wx2 or SP-Sephadex C25) before reduction separates the mixture of copper(II) complexes

(33) Comba, P.; Hambley, T. W.; Lawrance, G. A. *Helv. Chim. Acta* **1985**, *68*, 2332.
(34) Comba, P.; Hambley, T. W.; Lawrance, G. A.; Martin, L. L.; Renold, P.; Várnagy, K. *J. Chem. Soc., Dalton Trans.* **1991**, 277.
(35) Bernhardt, P. V.; Comba, P.; Hambley, T. W.; Martin, L. L.; Várnagy, K.; Zipper, L. *Helv. Chim. Acta* **1992**, *75*, 145.
(36) Balla, J.; Berhardt, P. V.; Buglyo, P.; Comba, P.; Hambley, T. W.; Schmidlin, R.; Stebler, S.; Várnagy, K. *J. Chem. Soc., Dalton Trans.* **1993**, 1143.
(37) Rosokha, S. V.; Lampeka, V. D.; Maloshtan, I. M. *J. Chem. Soc., Dalton Trans.* **1993**, 631.
(38) Bernhardt, P. V.; Hayes, E. J. *J. Chem. Soc., Dalton Trans.* **1998**, 3539.
(39) Bernhardt, P. V.; Comba, P.; Hambley, T. W.; Lawrance, G. A.; Várnagy, K. *J. Chem. Soc., Dalton Trans.* **1992**, 355.
(40) Bernhardt, P. V.; Comba, P. *Inorg. Chem.* **1993**, *32*, 2798.
(41) Comba, P. *Inorg. Chem.* **1994**, *33*, 4577.
(42) Comba, P.; Börzel, H.; Pritzkow, H.; Sickmüller, A. *Inorg. Chem.* **1998**, *37*, 3853.
(43) Comba, P.; Sickmüller, A. F. *Inorg. Chem.* **1997**, *36*, 4500.
(44) Comba, P. *Coord. Chem. Rev.* **1999**, *182*, 343.
(45) Bernhardt, P. V.; Comba, P.; Hambley, T. W. *Inorg. Chem.* **1993**, *32*, 2804.
(46) Bernhardt, P. V.; Comba, P. *Helv. Chim. Acta* **1991**, *74*, 1834.
(47) De Blas, A.; De Santis, G.; Fabbrizzi, L.; Licchelli, M.; Lanfredi, A. M. M.; Morosini, P.; Pallavicini, P.; Ugozzoli, F. *J. Chem. Soc., Dalton Trans.* **1993**, 1411.
(48) Xin, L.; Curtis, N. F.; Weatherburn, D. C. *Transition Met. Chem.* **1992**, *17*, 147.
(49) Hambley, T. W.; Lawrance, G. A.; Maeder, M.; Wilkes, E. N. *J. Chem. Soc., Dalton Trans.* **1992**, 1283.
(50) Baran, Y.; Lawrance, G. A.; Wilkes, E. N. *Polyhedron* **1997**, *16*, 599.
(51) Comba, P. In *Intermolecular Interactions*; Gans, W., Boeyens, J. C. A., Eds.; Plenum Press: New York, 1998; p 97.

into three purple bands. Zn/HCl reduction of each band, followed by ion exchange chromatography and ^{1}H NMR characterization of the resulting metal-free ligands, indicates that the third (small) fraction is due to pure $[Cu(a\text{-}pypymac)]^{2+}$; the others are syn/anti mixtures. Crystallization of the copper(II) compounds form the three fractions produces red and purple crystals; spectroscopic and crystallographic analyses (see below) indicate that some of these are N-based isomers. Note, that in acidic solutions there is partial interconversion of these isomers.

The synthesis of the cobalt(III) compounds involves the usual oxidation of the cobalt(II) precursors, obtained from a stoichiometric mixture of the metal-free ligand (fully protonated; syn/anti mixture, ratio 1:9), a cobalt(II) salt, and base, in the presence of charcoal.[52,53] Chromatographic separation of the product mixture on SP Sephadex C25 and Dowex 50Wx2 produces the pure $[Co(a\text{-}pypymac)]^{3+}$ and a mixture that probably includes $[Co(s\text{-}pypymac)]^{3+}$ and various aqua− and chloro−cobalt(III) complexes with tetra- and/or pentacoordinated pypymac. Isomerically pure $[Co(a\text{-}pypymac)]^{3+}$ and $[Co(s\text{-}pypymac)]^{3+}$ were obtained when water and chloride were excluded in the oxidation reaction to enforce hexacoordination of pypymac: a solution of the metal-free ligands (syn/anti mixture) in ethanol, produced by a catalytic reduction (Raney nickel) of the copper(II) precursor, to which cobalt(II)tetrafluoroborate was added in situ was oxidized in the presence of charcoal. Separation on SP Sephadex C25 produced two main yellow-orange fractions, $[Co(s\text{-}pypymac)]^{3+}$ and $[Co(a\text{-}pypymac)]^{3+}$, which were purified on Dowex 50Wx2. X-ray-quality single crystals of the chloride salt of the s-isomer were obtained by slow evaporation of the acidic aqueous solution; recrystallization of a microcrystaline product from water/$NaClO_4$ produced crystals of the a-isomer.

The perchlorate salt of $[Ni(a\text{-}pypymac)]^{2+}$ was crystallized from an aqueous solution of the pure a-pypymac ligand (fully protonated), 1 equiv of nickel(II) perchlorate, and base (pH = 9). For the synthesis of the zinc(II) compound the pure isomer of a-pypymac was neutralized (Amberlite RA 416). The free base was reacted with zinc(II) tetrafluoroborate, and $[Zn(a\text{-}pypymac)]^{2+}$ was crystallized as the hexafluorophosphate salt.

Isomerism of the Hexacoordinate Compounds. The three conformations each of $[M(a\text{-}pypymac)]^{n+}$ and $[M(s\text{-}pypymac)]^{n+}$ are shown in Chart 3a (amine protons omitted). Note that the nomenclature adoped here is not unambiguous;[42,54] the assignment of δ or λ conformation for each of the five-membered chelate rings depends on the orientation of the structural plots. The standard adopted here generally has a pendant pyridinyl group coordinated to the $+z$ axis and attached to the equatorial six-membered chelate ring on the left. We prefer this nomenclature to less widely used and less easy to visualize variants.[42,54] Note, also, that all six structures shown in Chart 3a are isomers.

$\delta\delta$- and $\lambda\lambda$-$[M(a\text{-}pypymac]^{n+}$ are degenerate, as are $\delta\lambda$- and $\lambda\delta$-$[M(s\text{-}pypymac)]^{n+}$. The idealized point groups of the six isomers are the following: $\delta\lambda$-$[M(a\text{-}pypymac)]^{n+}$, C_{2h}; $\lambda\delta$-$[M(a\text{-}pypymac)]^{n+}$, C_{2h}; $\delta\delta/\lambda\lambda$-$[M(a\text{-}pypymac)]^{n+}$, C_i; $\lambda\lambda$-$[M(s\text{-}pypymac)]^{n+}$, C_2; $\delta\lambda/\lambda\delta$-$[M(s\text{-}pypymac)]^{n+}$, C_s; $\delta\delta$-$[M(s\text{-}pypymac)]^{n+}$, C_2. The two most prominent structural parameters of diammac-type complexes are the axial bending θ for the anti isomers and the trigonal twist ϕ for the syn isomers (see Chart 3b). Also of interest for $[M(pypymac)]^{n+}$ are the two angles

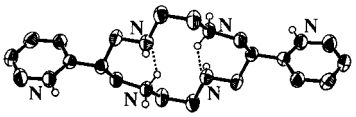

Figure 1. ORTEP[55] plot of $(a\text{-}pypymacH_4)(ClO_4)\cdot 2H_2O$.

Chart 3

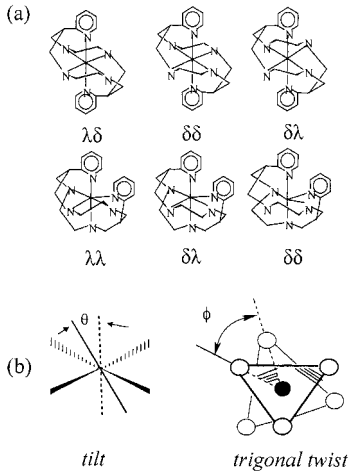

between the planes defined by each of the pyridine donors and that defined by the two secondary amine donors of the adjacent six-membered chelate ring and the metal center (α, ideally 90°) and the deviation of the trace of the pyridine rings in the plane defined by the two amine donors of the adjacent six-membered chelate ring and the metal center from the line defined by the metal ion and the centroid of the two corresponding secondary amine donors (γ, ideally 0°). Other coordination geometries of $[M(pypymac)]^{n+}$ compounds that have been observed are based on the four-coordinate ligand, with the two pendant pyridinyl donors not coordinated (e.g., copper(II) compounds), and complexes with five-coordinated pypymac. These are not considered in the structural discussion based on the force field calcualtions.

Solid State Structures. The metal-free a-pypymac ligand crystallizes as the tetrahydroperchlorate salt with two molecules of water (Figure 1). The structure has a center of symmetry at the centroid of the macrocyclic ring. The two pyridine nitrogen atoms and two of the secondary amine donors are protonated. In addition to intermolecular hydrogen bonds from the protonated amine and pyridine donors to the water molecules and perchlorate anions there are strong intramolecular hydrogen bonds between the two pairs of protonated/nonprotonated amine donors (N2−H···N1′ = 2.118 Å; see Figure 1). Together with these protons the pyridinyl-substituted diaminopropane "caps" build six-membered (chelate) rings which are in a chair conformation with equatorially disposed pyridinyl donors, leading to the stable pseudo-trans-III configuration of the tetraazamacrocycle. Hence, the ligand is in a highly preorganized conformation for metal ion coordination: the four amine donors are endocyclic, the four secondary amines as well as the central carbon atoms of the "caps" have the same configurations, and the preformed en-type chelate rings have the same conformation as in all known metal complexes with hexacoordinated a-pypymac (see discussion below). The only requirements for hexacoordination are reflections of the two pseudo-six-membered chelate rings and rotations around the C−C axes involving the pyridinyl groups by approximately 180°.

Two sets of crystals of the copper(II) compound of a-pypymac were isolated, purple $[Cu(a\text{-}pypymac)(ClO_4)_2]$ and violet $[Cu(a\text{-}pypymacH_2)(Cl)_2](ClO_4)_2$. One pair of amine donors in the

(52) Dwyer, F. P.; Sargeson, A. M. *Nature* **1960**, *187*, 1022.
(53) Comba, P.; Hambley, T. W.; Zipper, L. *Helv. Chim. Acta* **1988**, *71*, 1875.
(54) Bernhardt, P. V.; Byriel, K. A.; Kennard, C. H. L.; Sharpe, P. C. *Inorg. Chem.* **1996**, *35*, 2045.

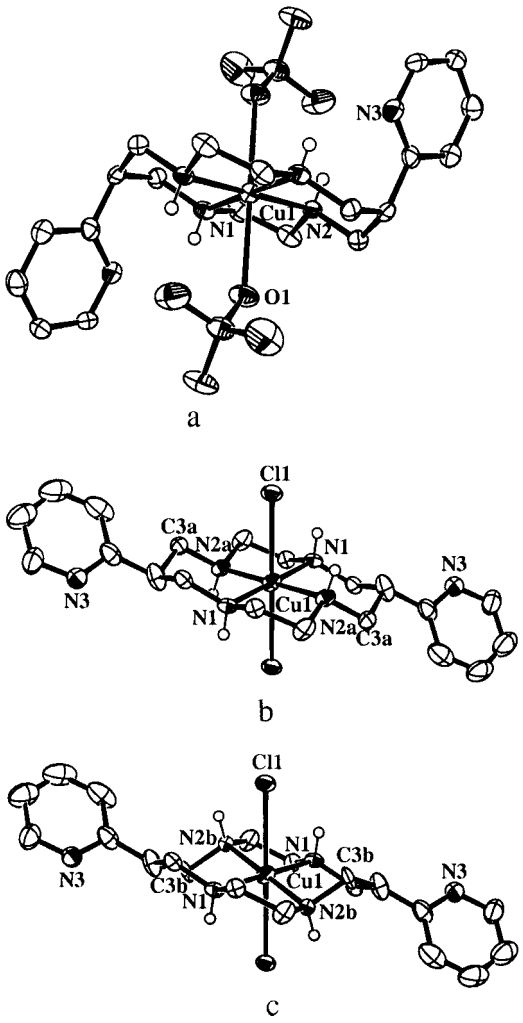

Figure 2. ORTEP[55] plots of (a) $[Cu(a\text{-}pypymac)(ClO_4)_2]$ and (b, c) the two geometries of the disordered structure of $[Cu(a\text{-}pypymacH_2)(Cl)_2](ClO_4)_2$.

latter, centrosymmetrical structure is disordered; the two not coordinated pyridinyl donors are protonated. The three molecular cations of the copper(II) compounds (two for the disordered structure) are shown in Figure 2, and relevant bond distances and valence angles are given in Table 1. The purple compound has two axial oxygen (perchlorate) donors at the expected distance of 2.603 Å; in the violet salt two chloride anions are coordinated at 2.835 Å (larger ionic radius). The perchlorate complex has the usual trans-III configuration, with the five-membered chelate rings in the expected δ/λ conformations and chair conformations of the two six-membered chelate rings. Note that reflection of the six-membered chelate rings to boat conformation would not lead to coordination of the pyridinyl donors; i.e., the central carbon atoms of the "caps" or all coordinated amines have inverted configurations (see discussion of the ligand structure above).

The configuration of the two models of the disordered structure of the violet compound are both different from that of the purple complex. One of the structures (Figure 2b, 70%) has the trans-III configuration and, as expected, the same δ/λ conformation of the five-membered chelate rings as the purple isomer and chair conformations of the six-membered chelate rings; relative to the purple isomer the central carbon atoms of the caps are inverted: the protonated pyridinyl groups are equatorial, i.e., similar to the structure of the metal-free ligand (see above). In the second structure (Figure 2c, 30%) one pair of symmetry-related amine donors is inverted, leading to the extremely rare trans-IV configuration, and the six-membered chelate rings are in twist-boat conformation, with very short Cu−N bonds to the inverted amines (1.949 Å; average 1.979 Å).

The structure of the molecular cation of $[Cu(s\text{-}pypymacH_2)(ClO_4)](ClO_4)_3$ is shown in Figure 3, and selected structural parameters are also given in Table 1. The macrocycle is found in the trans-I configuration; i.e., all amine protons are on the same side of the CuN4 plane. This configuration usually is found for ligands with substituted amines, leading to five-coordinate species, but with the axial ligand on the same side as the amine substituents. The bond to the axial perchlorate in this present example is 2.595 Å; there is some contact to a perchlorate oxygen on the other side with Cu−O = 2.877 Å. The six-membered chelate rings have chair conformations, and those of the five-membered chelate rings are δ/δ.

ORTEP[55] plots of the four molecular cations $[Co(a\text{-}pypymac)]^{3+}$, $[Co(s\text{-}pypymac)]^{3+}$, $[Ni(a\text{-}pypymac)]^{2+}$, and $[Zn(a\text{-}pypymac)]^{2+}$ are shown in Figure 4, and the relevant structural parameters are given in Table 2. The three structures with a-pypymac are very similar to each other, and all are $\delta\lambda$-$[M(a\text{-}pypymac)]^{n+}$ isomers. The pyridine rings are perpendicular to the central MN_4 planes and parallel to each other ($\alpha \sim 90°$, $\gamma \sim 0°$). The metal−donor distances are within the expected ranges for hexaamines ($N_4(py)_2$ donor sets) of the corresponding metal ions, and there are only minimal angular distortions; i.e., the coordination polyhedra are close to octahedral. The structure of $[Co(s\text{-}pypymac)]^{3+}$ has $\delta\delta$ conformation and bond distances that are typical for cobalt(III) hexaamines and similar to those of $[Co(a\text{-}pypymac)]^{3+}$ (i.e., the hole sizes of the two isomers seem to be similar.

Computed Structures and Strain Energies. Force field calculations with the MOMEC program[56] and force field[57] have been used to determine the rigity of the ligand, to predict the structures of hexacoordinated transition metal compounds of pypymac, to compute the stability of the various isomers as a function of the metal ion size, and to analyze the stress induced by the metal ion to the ligands and vice versa. These studies involved the following: (i) the refinement of all six isomers of $[M(pypymac)]^{n+}$ with M = Co^{3+}, Ni^{2+}, and Zn^{2+}, as well as Cr^{3+} and low-spin Fe^{3+} (the strain energies and selected structural parameters are presented in Table 3; the corresponding experimental structural data appear for comparison); (ii) the computation of the strain energies of the metal-free ligand as a function of the sum of all six distances of the donor atoms to a nonspecific metal ion (centroid of the cavity, metal-independent "hole size" calculations; see Figure 5 and Table 4);[58] (iii) a comparison of the structures of the metal ion-specific calculations (see part i and Table 3) and the metal-independent computations (see part ii and Table 4), where for each metal ion a comparison to the minimum of the corresponding curve is also given (see Table 5).

The agreement between the strain energy minimized and the experimental structures is satisfactory; for cobalt(III) it is excellent, for nickel(II) it is good, and for the less well refined force field of zinc(II) it is acceptable (see Table 3). The overall

(55) Johnson, C. K. *ORTEP, A Thermal Ellipsoid Plotting Program*; Oak National Laboratories: Oak Ridge, TN, 1965.
(56) Comba, P.; Hambley, T. W.; Okon, N.; Lauer, G. *MOMEC97 a molecular modeling package for inorganic compounds*; CVS: Heidelberg, Germany, 1997 (e-mail: cvs@t-online.de).
(57) Bol, J. E.; Buning, C.; Comba, P.; Reedijk, J.; Ströhle, M. *J. Comput. Chem.* **1998**, *19*, 512.
(58) Comba, P.; Okon, N.; Remenyi, R. *J. Comput. Chem.* **1999**, *20*, 781.

Table 1. Selected Bond Distances (Å) and Angles (deg) for [Cu(a-pypymac)$(ClO_4)_2$], [Cu(a-pypymac$H_2(Cl)_2$]$(ClO_4)_2$, and [Cu(s-pypymac$H_2(ClO_4)$]$(ClO_4)_3$

	[Cu(*a*-pypymac)$(ClO_4)_2$]	[Cu(*a*-pypymac$H_2(Cl)_2$]$(ClO_4)_2$	[Cu(*s*-pypymac$H_2(ClO_4)$]$(ClO_4)_3$
Cu1−N1	2.010(4)	2.008(3)	2.003(5); Cu1−N3, 1.984(5)
Cu1−N2 (N2B; N2A)	2.025(4)	1.949(11); 2.049(4)	2.007(5); Cu1−N4, 2.010(5)
Cu−X (O1; Cl1)	2.603[a]	2.835(3)[b]	2.595[c]
N−Cu1−N2 (5-membered ring)	84.41(17)	86.3(3) (87.39(11))	87.5(2) (86.9(2))
N−Cu1−N2 (6-membered ring)	93.59(17)	93.7(3) (92.61(11))	94.5(2) (93.1(2))
N−Cu1−N2 (trans)	180.0	179.999(2) (180.0)	170.1(2) (168.7(2))

[a] Two perchlorate O. [b] Two Cl^-. [c] One perchlorate O.

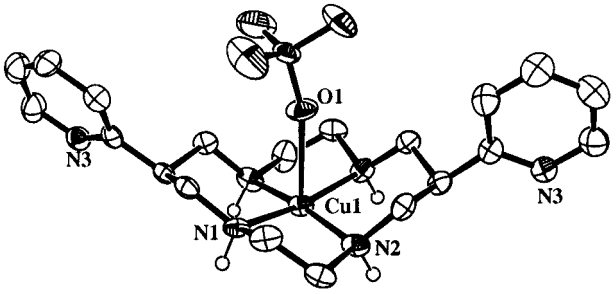

Figure 3. ORTEP[55] plot of [Cu(s-pypymacH_2)(ClO_4)]$(ClO_4)_3$.

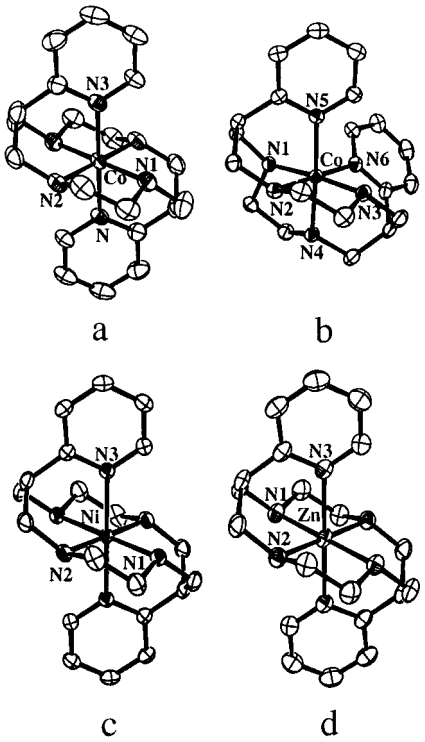

Figure 4. ORTEP[55] plots of the molecular cations of (a) [Co(a-pypymac)]$(ClO_4)_3$, (b) [Co(s-pypymac)]Cl_3, (c) [Ni(a-pypymacH_4)]-$(ClO_4)_2$, and (d) [Zn(a-pypymac)]$(PF_6)_2$.

picture is that the structures (experimental and computed) are rather symmetrical with the expected angles for five-membered chelate rings (approximately 85°) and six-membered chelate rings (approximately 95°), trans angles close to 180°, little deviation of the apical donors from the *z*-axis ($\theta \sim 90°$), and little trigonal distortion ($\phi \sim 55°$); also, the orientation of the pyridine rings is nearly ideal ($\alpha \sim 90°$, $\gamma \sim 0°$). This is expected from the hole size calculations. One conformation each (a-pypymac, $\delta\lambda$; s-pypymac, $\delta\delta$) is preferred over the whole range ($M-N_{average} = 1.9-2.4$ Å). The optimum size of the metal ion ($M-N_{average}$ distance) is nearly identical for the two isomers (approximately 2.13 Å) and slightly larger than for the amine analogue diammac.[46,59] The extra carbon atom between the macrocyclic backbone and the donor of the pendant group leads to little distortion from octahedral geometry and rather flat strain energy vs metal ion size curves (Figure 5, Tables 4 and 5). From the hole size calculations it appears that the cavity size for s-pypymac is slightly smaller than for a-pypymac (Figure 5, Table 5) and that, for M−L elongations, the syn isomer is less flexible than the anti isomer, while, for M−L compression, the anti isomer is less flexible than the syn isomer. An interesting feature is that, for cobalt(III), the anti isomer is less stable than the syn isomer, and this is the result of ligand strain (see Table 5).

On the basis of the force field calculations (hole size calculations; see Figure 5 and Table 4), the ligand preference for a-pypymac is for the $\delta\lambda$-conformation with an average M−N distance of 2.13 Å ($M-N_{amine} = 2.08$ Å, $M-N_{pyridine} = 2.22$ Å). From the experimental and computed structural data it appears that cobalt(III) is too small (i.e. the ligand enforces an M−N elongation;[44] average $Co^{III}-N = 1.97$ Å (calcd 1.96 Å), $Co^{III}-N_{amine} = 1.98$ Å, and $Co^{III}-N_{pyridine} = 1.95$ Å (note that there is an electronically enforced inversion of the $Co^{III}-N_{amine}/N_{pyridine}$ ratio); ligand strain 27 kJ/mol, CoN_6 strain 34 kJ/mol). The nickel(II) ion is also slightly too small (average $Ni^{II}-N =$ 2.10 Å (calcd 2.07 Å); $Ni^{II}-N_{amine} = 2.08$ Å, $Ni^{II}-N_{pyridine} =$ 2.13 Å; ligand strain 5 kJ/mol, NiN_6 strain 15 kJ/mol). The size of the zinc(II) ion is close to ideal (note, however, that the ligand-preferred $M-N_{amine}/M-N_{pyridine}$ ratio is slightly different; average $Zn^{II}-N = 2.16$ Å (calcd 2.13 Å); $Zn^{II}-N_{amine} = 2.11$ Å, $Zn^{II}-N_{pyridine} = 2.24$ Å; ligand strain 1 kJ/mol, ZnN_6 strain 18 kJ/mol). The conformation of the $[Co(s\text{-pypymac})]^{3+}$ complex is $\delta\delta$ (note that for *cis*-diammac the $\lambda\lambda$ conformation is expected[46] and observed;[39,45] only small distortions from octahedral coordination geometry ($\phi = 0°$)). Note that on the basis of the force field calculations $\delta\delta$-$[Co(s\text{-pypymac})]^{3+}$ is more stable than $\delta\lambda$-$[Co(a\text{-pypymac})]^{3+}$ ($\Delta U = 6$ kJ/mol; see Table 3).

Solution Structures and Properties. (a) NMR Spectroscopy of the Metal-Free Ligand. The fact that in the ^{13}C NMR spectrum of a-pypymac there are five signals for the pyridinyl substituents and only three at higher field (methylene groups) might indicate that the symmetry in solution is higher than in the solid state (see Figure 1; C_{2h} vs C_i); that is, there is a fast proton exchange between the two amine sites within the pseudo six-membered rings. The ^1H NMR signals were fully assigned on the basis of H,C-COSY and DEPT spectra (see Supporting Information). From a simulation of the AA′XX′ pattern for the protons of the ethylene bridge (en rings; see Supporting Information) there results a geminal coupling constant of $^2J_{AX} = -13.4$ Hz and three vicinal coupling constants of $^3J_{AA'} =$ 11.8 Hz, $^3J_{AX'} = 3.0$ Hz, and $^3J_{XX'} = 3.7$ Hz. On the basis of the crystallographically determined H−C−C−H torsional angles

(59) Comba, P.; Hambley, T. W. *Molecular Modeling of Inorganic Compounds*; VCH: Weinheim, Germany, 1995.

Table 2. Selected Bond Lengths (Å) and Angles (deg) of [Co(s-pypymac)]$(Cl)_3$, [Co(a-pypymac)]$(ClO_4)_3$, [Ni(a-pypymac)]$(ClO_4)_2$, and [Zn(a-pypymac)]$(PF_6)_2$

	[Co(*s*-pypymac)]$(Cl)_3$	[Co(*a*-pypymac)]$(ClO_4)_3$	[Ni(*a*-pypymac)]$(ClO_4)_2$	[Zn(*a*-pypymac)]$(PF_6)_2$
M−N1	1.969(3)	1.991(3)	2.088(3)	2.1232(19)
M−N2	1.981(3)	1.972(3)	2.08(3)	2.102(2)
M−N3	1.986(3)	1.948(3)	2.127(2)	2.2445(19)
M−N4	1.986(3)		2.078(3)	
M−N5	1.960(3)		2.093(3)	
M−N6	1.952(3)		2.138(2)	
N2−M−N1	90.99(13)	84.82(13)	85.63(10)	85.74(8)
N2−M−N3	85.85(13)	88.40(13)	86.82(10)	85.89(8)
N1− M−N3	175.57(13)	90.85(13)	93.53(10)	93.93(8)
N4−M−N5	177.12(13)		85.68(10)	
N4−M−N6	88.62(13)		93.32(10)	
N5−M−N6	92.66(13)		86.01(10)	

Table 3. Observed and Computed Structural Parameters and Strain Energies of $[M(pypmac)]^{n+}$ (Distances in Å, Angles in deg, and Energies in kJ/mol; Experimental Data in Parentheses)

compound		$M-N_{amine}$[a]	$M-N_{pyridin}$[a]	$N_{py-}M-N_{py}$[a]	$N_{A-}M-N_A$[a]	$N_{py-}M-N_A$[a]	θ (Ø)[b,c]	α[b]	γ[b]	U_{strain}
					a-pypymac					
Cr^{III}	$\delta\lambda$	2.07	2.04	180	86, 94, 180	88, 92	87	90	0.0	81.6
	$\delta\delta/\lambda\lambda$	2.05	2.07	176	89, 91, 175	88, 96, 89, 87	87	85	8.5	98.4
	$\lambda\delta$	2.03	2.10	180	91, 89, 180	94, 86	84	90	0.0	138.3
lsFe^{III}	$\delta\lambda$	2.00	1.98	180	86, 94, 180	88, 92	87	90	0.0	102.9
	$\delta\delta/\lambda\lambda$	1.98	2.01	176	89, 91, 175	88, 96, 89, 87	88	84	8.5	116.0
	$\lambda\delta$	1.97	2.03	180	91, 89, 180	94, 86	84	90	0.0	155.7
Co^{III}	$\delta\lambda$	1.97 (1.97, 1.99)	1.94 (1.95)	180 (180)	86, 94, 180 (85, 95, 180)	88, 92 (88, 89, 92, 91)	88 (88)	90 (90)	0.2 (2.3)	122.8
	$\delta\delta/\lambda\lambda$	1.96	1.96	176	89, 92, 175	88, 96, 89, 87	88	84	8.5	135.5
	$\lambda\delta$	1.94	1.99	180	90, 90, 180	94, 86	85	90	0.0	176.0
Ni^{II}	$\delta\lambda$	2.08 (2.08, 2.09)	2.09 (2.14)	180 (180)	86, 94, 180 (86, 96, 180)	88, 92 (86, 87, 94, 93)	87 (85)	90 (90)	0.0 (0.0)	77.9
	$\delta\delta/\lambda\lambda$	2.04	2.12	176	89, 91, 175	88, 95, 89, 88	88	84	9.0	93.1
	$\lambda\delta$	2.01	2.16	180	91, 88, 180	94, 86	84	90	0.0	129.8
Zn^{II}	$\delta\lambda$	2.15 (2.10, 2.12)	2.12 (2.24)	180 (180)	85, 95, 180 (86, 96, 180)	88, 92 (86, 94)	88 (84)	90 (87)	0.0 (1.2)	76.5
	$\delta\delta/\lambda\lambda$	2.10	2.18	174	88, 92, 175	89, 91, 87, 87	85	84	10.5	93.6
	$\lambda\delta$	1.06	2.24	180	91, 89, 180	97, 83	81	90	0.3	128.7
					s-pypymac					
Cr^{III}	$\delta\delta$	2.08, 2.07	2.02	92	85, 89, 172, 92	88, 91, 177	52	88	3.5	77.2
	$\lambda\delta/\delta\lambda$	2.08, 2.07	2.03	93	85, 86, 87, 93, 172, 88	86, 86, 87, 95, 171, 169	(59)	84, 89	10.2	83.7
	$\lambda\lambda$	2.09, 2.05	2.03	93	86, 94, 180, 83	84, 93, 169	58	82	10	93.1
lsFe^{III}	$\delta\delta$	2.00, 2.00	1.97	89	86, 89, 193, 93	89, 92, 178	54	88	4	97.7
	$\lambda\delta/\delta\lambda$	2.00, 2.00	1.99	90	86, 87, 86, 97, 173, 89	87, 88, 88, 96, 172, 171	(59)	84, 90	10.0	104.2
	$\lambda\lambda$	2.09, 1.98	1.98	91	87, 95, 178, 84	85, 93, 172	58	82	9	111.5
Co^{III}	$\delta\delta$	1.98, 1.97 (1.98, 197)	1.93 (1.95, 1.96)	89 (93)	86, 89, 173, 92 (86, 91, 176, 91)	89, 93, 178 (88, 92, 177)	54 (55)	88 (81, 87)	5 (5.8)	116.1
	$\lambda\delta/\delta\lambda$	1.97, 1.97	1.94	90	86, 87, 87, 98, 173, 88	86, 89, 88, 96, 172, 172	(57)	84, 89	10.0	123.1
	$\lambda\lambda$	1.98, 1.98	1.94	91	87, 94, 178, 84	86, 93, 173	56	83	9	129.5
Ni^{II}	$\delta\delta$	2.09, 2.10	2.06	92	85, 89, 172, 92	88, 91, 176	52	88	3	74.2
	$\lambda\delta/\delta\lambda$	2.09, 2.06	2.08	93	85, 86, 87, 98, 172, 88	85, 86, 87, 95, 169, 171	(57)	84, 88	10.2	80.4
	$\lambda\lambda$	2.10, 2.04	2.08	93	86, 94, 180, 83	84, 93, 169	56	81	10	89.7
Zn^{II}	$\delta\delta$	2.19, 2.22	2.08	98	82, 86, 164, 89	87, 90, 172	48	88	3	69.4
	$\lambda\delta/\delta\lambda$	2.19, 2.22	2.12	98	82, 83, 84, 95, 174, 85	84, 86, 86, 93, 163, 168	(53)	84, 86	9, 4	75.0
	$\lambda\lambda$	2.23, 2.14	2.13	98	82, 91, 172, 79	82, 93, 163	52	80	11	85.0

[a] Averages of symmetry-related parameters. [b] For definition of the structural parameters see Chart 3b and text. [c] Anti isomer, θ; syn isomer, ϕ.

of 172.1, 59.1, and 55.8°, the expected coupling constants (Karplus relation) are 10−15 and 3−4 Hz; that is, the solution structure is similar to that observed in the crystal lattice. This is in contrast to the ^{1}H NMR spectra of *cis*- and *trans*-diammacH_4^{4+} (see Chart 1), where the observation of simple singlets leads to the interpretation that there is a fast equilibrium between the two conformers with axial and equatorial ammonia substituents.[39] The corresponding bis(ethyl/amine)-substituted metal-free ligand (anti isomer) has an AA′BB′ coupling pattern for the ethyl bridges;[54] that is, the size of the substituents might be of importance for the conformational stability.

(b) NMR Spectra of the Cobalt(III) Complexes. NMR spectra have also been used to analyze the structures of [Co(a-pypymac)]$^{3+}$ and [Co(s-pypymac)]$^{3+}$ in solution (see Chart 4). From the ^{13}C NMR spectra it emerges that the two isomers have the expected symmetry (anti, C_{2h}, four resonances at low field (pyridine, one signal not resolved), three resonances at higher field (aliphatic carbon atoms); syn, C_2 symmetry, five

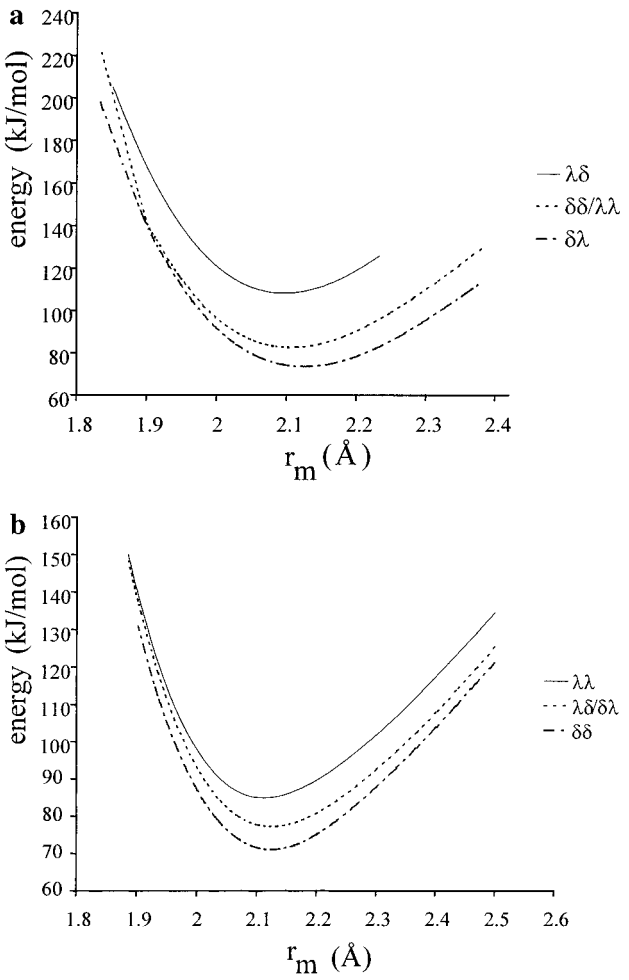

Figure 5. Hole size curves (strain energy vs averaged metal−donor bond distances, constrained sum) of (a) $[M(a\text{-pypymac})]^{n+}$ and (b) $[M(s\text{-pypymac})]^{n+}$.

signals at low field (pyridine), five signals at higher field (aliphatic carbon atoms); see Experimental Section). The assignment of the ^{1}H NMR signals is based on H,H- and H,C-COSY experiments (see Supporting Information). As expected from the force field calculations, the ^{1}H NMR spectrum of $[Co(a\text{-pypymac})]^{3+}$ (see Supporting Information) is that of a pure isomer; in the spectrum of $[Co(s\text{-pypymac})]^{3+}$ some minor amounts of the less abundant isomers are visible ($\delta\delta$:$\delta\lambda/\lambda\delta$:$\lambda\lambda$ ≅ 94:5:1; see above). Protons 1−3 (A,B,C) of $[Co(a\text{-pypymac})]^{3+}$ (see Chart 4) exhibit an ABX coupling pattern with $^2J_{2,3} = -13.5$ Hz, $^3J_{1,2} = 3.8$ Hz, and $^3J_{1,3} = 1.7$ Hz. Protons 4−7 (D,E,D′,E′) lead to a AA′XX′ spin system with $^3J_{5,6} = 13.9$ Hz, $^3J_{5,7} = {}^3J_{4,6} = 3.9$ Hz, $^3J_{4,7} = 1.0$ Hz, and $^2J_{4,5} = {}^2J_{6,7} = -13.0$ Hz. The corresponding torsional angles from the solid-state structure are 173.7, 53.6, and 66.2°, and from the Karplus relation the calculated coupling constants are in the expected ranges ($^3J_{5,6} = 10-15$ Hz, $^3J_{5,7} = {}^3J_{4,6} = 3-5$ Hz, $^3J_{4,7} = 1-2$ Hz). Thus, as expected on the basis of the force field calculations, the solution structure is similar to that in the solid state, i.e., $\delta\lambda$-$[Co(a\text{-pypymac})]^{3+}$.

(c) Solution Electronic Spectra of $[Cu(a\text{-pypymac})]^{2+}$. Ion exchange chromatography of $[Cu(pypymac)]^{2+}$ with a 9:1 mixture of the anti and syn isomers of the macrocyclic ligand indicates that at least three isomeric forms of the copper(II) compound are present in solution. These are N-based isomers and/or isomers based on the orientation of the pyridinyl substituent at the six-membered chelate rings (axial vs equatorial). We anticipate that the three fractions include the three isomers of $[Cu(a\text{-pypymac})]^{2+}$, characterized crystallographically (see Figure 2), apart from minor amounts of the isomers of s-pypymac complexes (Figure 3; note that a thorough and quantitative analysis is not possible due to isomer interconversion in the acidic solutions resulting from the elution from Dowex 50Wx2).

Electronic spectra of the two pure, crystalline isomers ($[Cu(a\text{-pypymac})(ClO_4)_2]$, purple crystals; $[Cu(a\text{-pypymacH}_2)(Cl)_2](ClO_4)_2$, violet crystals) were recorded at two pH values (pH 7, fully deprotonated coordinated ligand; pH 1, two protonated pyridine donors each; see experimental and Supporting Information for spectroscopic parameters and for preliminary potentiometric titration data). For the deprotonated violet complex (see Figure 2b,c), compared to the deprotonated purple complex (see Figure 2a), there is a shift of the d−d transition of 380 cm^{-1} toward lower energy (both solutions at pH 7). Protonation (noncoordinated pyridine donors) of both compounds leads to a shift of the d−d transition toward lower energy (500 and 330 cm^{-1}, for the purple and violet compounds, respectively). Similar effects have been observed for other copper(II) compounds with noncoordinated pendant groups, and various interpretations have been offered.

The two trans-III isomers of $[Cu(anti\text{-diMeammac})(OH_2)]^{2+}$ (diMeammac = 6,13-bis(dimethylamino)-6,13-dimethyl-1,4,8,-11-tetraazacyclotetradecane, i.e., the dimethyl-substituted diammac derivative; see Chart 1) with axial or equatorial dimethylamino groups have a difference in the d−d transition of 436 cm^{-1}; the absorption maximum of the isomer with axial noncoordinated pendant amines (similar to our purple isomer, Figure 2a) is at higher energy (497 nm vs 508 nm).[60,61] A structural and spectroscopic analysis that involved AOM calculations led to the conclusion that the shift in transition energy was not due to changes in the coordination geometry; it was attributed to hydrogen bonding in the compound with axial dimethylamines that involves the protons of the coordinated amines and the methylated dangling amine, leading to an increasing nucleophilicity of the secondary amine donors and therefore to a higher ligand field.[60,61]

pH-dependent electronic properties (shifts of the d−d transition of up to approximately 960 cm^{-1}, higher energy at higher pH) were observed with various copper(II) and similar nickel(II) compounds with noncoordinated protonatable side chains.[30,60−63] This effect was interpreted with hydrogen bonding of the protonated side chains to the axial donors.[60−63] An alternative interpretation is based on electrostatic effects (charged pendant groups), and this is believed to be of some relevance with respect to biological systems.[30]

On the basis of the data available, a thorough interpretation of the pH-dependent shifts in the electronic spectra is not warranted. The solution spectroscopic parameters support the assumption that, upon dissolution in water and dilute acid, there are no severe structural changes with respect to the experimental solid state structures (see Figures 2 and 3); i.e., as expected, there is no inversion of the coordinated amines. This supports the model used to interpret the disorder of the structure with the partially protonated ligand.

(60) Bernhardt, P. V. *J. Chem. Soc., Dalton Trans.* **1996**, 4319.
(61) Bernhardt, P. V.; Hetherington, J. C.; Jones, L. A. *J. Chem. Soc., Dalton Trans.* **1996**, 4325.
(62) Tysmbal, L.; Rosokha, S. V.; Lampeka, Y. D. *J. Chem. Soc., Dalton Trans.* **1995**, 2633.
(63) Fabbrizzi, L.; Lanfredi, A. M. M.; Pallavicini, P.; Perotti, A.; Taglietti, A.; Ugozzoli, F. *J. Chem. Soc., Dalton Trans.* **1991**, 3263.

Table 4. Structural Parameters and Ligand-Based Strain Energies of pypymac as a Function of the Ligand Hole Size (Distances in Å, Angles in deg, and Energies in kJ/mol)

isomer	$\sum$M−N[a]	M−N_{amine}	M−$N_{pyridine}$	N_{py}−M−N_{py}	Θ	U_{strain}
			a-pypymac			
a-$\delta\lambda$ (min)	12.76	2.08	2.22	180	85	73.4
a-$\delta\delta/\lambda\lambda$		1.98, 2.05	2.40	174	89	82.8
a-$\lambda\delta$		1.96	2.46	180	86	109.2
a-$\delta\lambda$	12.64	2.07	2.18	180	86	73.8
a-$\delta\delta/\lambda\lambda$ (min)		1.97, 2.03	2.36	174	89	82.4
a-$\lambda\delta$		1.95	2.43	180	85	108.3
a-$\delta\lambda$	12.59	2.06	2.17	180	86	74.2
a-$\delta\delta/\lambda\lambda$		2.03, 1.97	2.35	174	89	82.5
a-$\lambda\delta$ (min)		1.94	2.41	180	85	108.2
a-$\delta\lambda$ (Co^{III})	11.82	1.97 (1.98)	1.99 (1.95)	180 (180)	87 (88)	101.9
a-$\delta\delta/\lambda\lambda$		1.88, 1.92	2.16	175	89	106.4
a-$\lambda\delta$		1.84	2.23	180	85	130.9
a-$\delta\lambda$ (Ni^{II})	12.62	2.07 (2.09)	2.18 (2.14)	180 (180)	86 (85)	74.0
a-$\delta\delta/\lambda\lambda$		1.97, 2.03	2.36	174	89	82.5
a-$\lambda\delta$		1.94	2.42	180	85	108.2
a-$\delta\lambda$ (Zn^{II})	12.94	2.10 (2.11)	2.27 (2.24)	180 (180)	85 (84)	74.2
a-$\delta\delta/\lambda\lambda$		2.03, 2.11	2.88	165	83	84.8
a-$\lambda\delta$		1.98	2.52	180	86	112.1
a-$\delta\lambda$	11.5	1.86, 1.93, 1.91, 1.90	1.87, 2.07	175	87	130.8
a-$\delta\delta/\lambda\lambda$		1.86, 1.84	2.10	176	89	132.0
a-$\lambda\delta$		1.79	2.16	180	85	157.1
a-$\delta\lambda$	13.4	2.13	2.44	180	83	82.5
a-$\delta\delta/\lambda\lambda$		2.01, 2.10	2.63	169	86	95.9
a-$\lambda\delta$		2.01	2.69	180	88	125.8
			s-pypymac			
s-$\delta\delta$ min	12.75	2.12, 2.17	2.09	94		85.0
s-$\delta\lambda/\lambda\delta$		2.00, 2.10, 2.10, 2.15	2.22, 2.19	92		77.2
s-$\lambda\lambda$		1.96, 2.16	2.26	93		71.0
s-$\delta\delta$ (Co^{III})	11.81	1.97, 2.01	1.92	90		97.8
s-$\delta\lambda/\lambda\delta$		1.90, 1.95, 1.95, 2.01	2.04, 1.96	89		103.8
s-$\lambda\lambda$		1.84, 2.01	2.05	90		107.6
s-$\delta\delta$	11.5	1.92, 1.96	1.87	89		122.0
s-$\delta\lambda/\lambda\delta$		1.86, 1.90, 1.90, 1.95	1.99, 1.90	88		128.5
s-$\lambda\lambda$		1.79, 1.96	2.00	89		130.8
s-$\delta\delta$	13.4	2.19, 2.22, 2.27, 2.23	2.22, 2.26	97		78.7
s-$\delta\lambda/\lambda\delta$		2.06, 2.21, 2.19, 2.21	2.33, 2.40	96		84.0
s-$\lambda\lambda$		2.05, 2.23	2.43	98		93.0

[a] Ranges of the calculations (11.5−13.4 Å), minima of the computed curves, and X-ray data (see first column).

Table 5. Comparison of the Computed Structures of Metal Ion-Independent and Metal Ion-Specific Structure Optimizations (in Å, Averages Where Appropriate)

param[a]	$\delta\delta$-[Co(*s*-pypy mac)]$^{3+}$	$\delta\lambda$-[Co(*a*-pypym ac)]$^{3+}$	$\delta\lambda$-[Ni(*a*-pypym ac)]$^{2+}$	$\delta\lambda$-[Zn(*a*-pypymac)]$^{2+}$
M−N_{amine}				
X-ray	1.98	1.97, 1.99	2.08, 2.09	2.10, 2.12
MM M-dep	1.97	1.97	2.08	2.15
MM M-indep	2.12, 2.17	2.08	2.08	2.08
M−pyridine				
X-ray	1.95	1.95	2.14	2.24
MM M-dep	1.93	1.94	2.09	2.13
MM M-indep	2.09	2.22	2.22	2.22

[a] M-dep, parameters from the optimized metal complexes; M-indep, minima of the corresponding hole size curves.

Chart 4

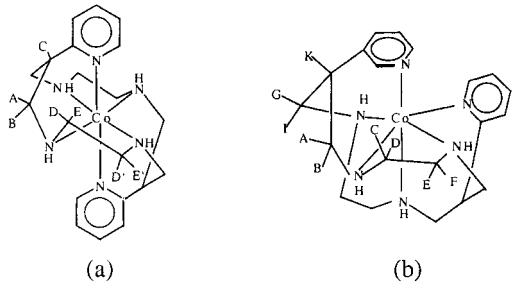

(a) (b)

Experimental Section

Materials. All reactions employed AR grade chemicals and solvents as supplied; solvents were dried with standard methods. Ethyl 2-pyridyl acetate was prepared as described (yield: 65%).[64] Raney alloy W2 was prepared according to the literature.[65]

Physical Methods. ^{1}H and ^{13}C NMR spectra at 500 (^{1}H) and 75.47 (^{13}C) MHz, respectively, were measured with Bruker WH 300 or Bruker Spectrospin DRX 500 instruments. Electronic spectra were obtained with a Varian Cary 2300 or a Varian Cary IE instrument. Cyclic voltammograms were recorded on a BAS 100B system, using 1×10^{-3} mol dm^{-3} solutions of the copper(II) compounds in a 0.1 mol dm^{-3} solution of KCl at a glassy carbon electrode, with an Ag/AgCl reference electrode and a Pt wire as the auxiliary electrode. All solutions for electrochemistry were purged with Ar before measurement. Potentiometric titrations were performed in aqueous solutions, using a combined

(64) Goldberg, N. N.; P. B. M.; Levine, R. *J. Am. Chem. Soc.* **1953**, *75*, 3843.
(65) Bauer, H. F.; Drinkard, W. C. *Inorg. Synth.* **1966**, 202.

Table 6. Crystal Data

	(a-pypymacH$_4$)(Cl O$_4$)$_4$·2H$_2$O	[Cu(a-pypymac) (ClO$_4$)$_2$]	[Cu(a-pypymacH$_2$(Cl$_2$)](ClO$_4$)$_2$	[Cu(*s*-pypymac)(ClO$_4$)](ClO$_4$)$_3$
space group	$P\bar{1}$	*Pbca*	$P2_1/a$	$P2_12_12_1$
formula	$C_{20}H_{38}Cl_4N_6O_{18}$	$C_{20}H_{30}Cl_2CuN_6O_8$	$C_{20}H_{36}Cl_4CuN_6O_{10}$	$C_{20}H_{34}Cl_4CuN_6O_{17}$
a, Å	8.501(4)	11.837(6)	14.824(7)	8.0146(9)
b, Å	9.796(5)	13.767(7)	6.654(3)	15.2449(17)
c, Å	11.442(6)	15.306(8)	14.959(7)	25.821(3)
α, deg	67.43(3)	90	90	90
β, deg	75.54(3)	90	98.74(3)	90
γ, deg	82.25(3)	90	90	90
V, Å^3	851.2(7)	2494(2)	1458.4(2)	3154.9(6)
Z	1	4	2	4
T, °C	21	−70	−70	−100
λ, Å	0.710 73	0.710 73	0.710 73	0.710 73
μ, mm^{-1}	0.431	1.149	1.178	1.117
d_{calc}, g/cm^3	1.546	1.643	1.653	1.760
R_1[a]	0.0564	0.0478	0.0578	0.0527
wR_2[a]	0.167	0.1135	0.1373	0.1216

	[Co(s-pypymac)]C l$_3$	[Co(a-pypymac)](ClO$_4$)$_3$	[Ni(a-pypymac)](Cl O$_4$)$_2$	[Zn(a-pypymac)](PF$_6$)$_2$
space group	$P2_1/c$	C_2/c	$P\bar{1}$	$P\bar{1}$
formula	$C_{20}H_{40}Cl_3CoN_6O_5$	$C_{20}H_{30}Cl_3CoN_6O_{12}$	$C_{20}H_{30}Cl_2N_6NiO_8$	$C_{20}H_{30}F_{12}N_6P_2Zn$
a, Å	8.873(4)	16.180(8)	8.423(6)	8.604(4)
b, Å	33.289(17)	11.705(6)	8.521(4)	8.938(4)
c, Å	9.200(5)	15.048(8)	18.253(4)	10.090(5)
α, deg	90	90	77.03(2)	113.86(3)
β, deg	98.05(3)	109.70(2)	78.32(2)	105.17(3)
γ, deg	90	90	78.45(2)	96.70(3)
V, Å^3	2691(2)	2683(2)	1233.7(10)	662.8(5)
Z	4	4	2	1
T, °C	−70(2)	−70(2)	−70(2)	−70(2)
λ, Å	0.710 73	0.710 73	0.710 73	0.710 73
μ, mm^{-1}	0.978	1.014	1.062	1.156
d_{calc}, g/cm^3	1.506	1.762	1.648	1.778
R_1[a]	0.0497	0.0503	0.0377	0.0341
wR_2[a]	0.1478	0.1475	0.0955	0.0877

[a] $R_1 = (\sum||F_o| - |F_c||)/\sum|F_o|$; w$R_2 = [(\sum w(F_o^2 - F_c^2)^2)/\sum w(F_o^2)^2]^{1/2}$.

glass electrode (Metrohm 6.0222.100) with an internal Ag/AgCl reference electrode, connected to a pH-Meter Metrohm 713. Addition of standard base (0.1 M KOH) was performed with a piston buret Dosimat 665 (Metrohm). All measurements were fully automated. The ionic strength was adjusted to 0.1 M, using KCl (metal-free ligand, Co(II), Zn(II), and Cd(II)) or KNO_3 (Hg(II)). All measurements were carried out at 25 °C under N_2 or Ar. Solutions of a-pypymac·6HCl (5×10^{-2} dm^{-3}, 10^{-3} mol dm^{-3}) alone and in the presence of 1 equiv of metal ion were titrated with 100 increments (4×10^{-5} dm^{-3}) of standard base (0.1 M KOH). The stability of the standard electrode potential (deviations less than 0.002 V) and the pK_w (13.79 ± 0.01) were checked by calibration titrations prior and after the measurements. Equilibrium constants were calculated from the potentiometric data using the programs SUPERQUAD[66] and BEST.[67] SUPERQUAD was used for the determination of the species involved; final refinements of the constants obtained with SUPERQUAD were carried out using BEST. Elemental analyses were performed by the microanalytical laboratory of the chemical institutes of the University of Heidelberg.

Structure Determination. Reflections of representative crystals were measured at the temperature given in Table 6. Intensity measurement data were obtained from a Siemens STOE-AED2 diffractometer, using Mo K$_\alpha$ radiation and operating in the *ω*-scan mode. The structures were solved by direct methods (SHELXS86) and refined by full-matrix least-squares methods based on F2 (SHELXL93), using anisotropic thermal parameters for all non-hydrogen atoms. All hydrogen atoms were located in a difference Fourier map and refined isotropically. Crystallographic data are given in Table 6.

Syntheses. *Caution! Perchlorate salts of metal complexes are potentially explosive. Although we did not experience any problems, these compounds should be handled extremely carefully.*

The template reaction, using 1 equiv of $Cu(NO_3)_2$·3H$_2$O, 2 equiv of 1,2-diaminoethane, 5 equiv of paraformaldehyde, 2 equiv of ethyl 2-pyridyl acetate, and triethylamine as base (3.3 equiv) in methanol yields the following products (separation on SP Sephadex C25, 25 × 7 cm, 0.2 M $NaClO_4$; see Chart 1 for ligand abbreviations): [Cu(s/a-pypymac)](ClO$_4$)$_2$ (<1%); [Cu(L^3)](ClO$_4$)$_2$ (11.2%); [Cu(L^1)$_2$] (35%); [Cu(L^2)](ClO$_4$) (4.5%). The side products were characterized by X-ray crystallography (see Figure 2; [Cu(L^3)](ClO$_4$) was reduced to L^4 (Zn/HCl) and coordinated to cobalt(III)). The template reaction around cobalt(II), aerobic conditions, with DBU as base yields a derivative of L^2 (diacid), coordinated to cobalt(III) in 27.4% yield; the crystal structural analysis of this compound is given in the Supporting Information.

(a) Bis(perchlorato)[*anti*-6,13-bis(2-pyridinyl)-1,4,8,11-tetraazacyclotetradecane]copper(II), (b) Dichloro[*syn*-6,13-bis(2-hydropyridinyl)-1,4,8,11-tetraazacyclotetradecane]copper(II) Diperchlorate, and (c) [Dichloro[*anti*-6,13-bis(2-hydropyridinyl)-1,4,8,11-tetraazacyclotetradecane]copper(II) Diperchlorate. To a stirred solution of $Cu(NO_3)_2$·3H$_2$O (3.66 g, 15.15 mmol) in methanol (30 mL) was added slowly a mixture of 1,2-diaminoethene monohydrate (2.36 g, 30.21 mmol). The resulting purple suspension was stirred for 1 h. Ethyl 2-pyridyl acetate (5.0 g, 30.27 mmol), DBU (40.0 g, 262.74 mmol), and paraformaldehyde (0.6 g, 20 mmol) were then added. The mixture was heated to 70 °C, and paraformaldehyde (2.4 g, 80 mmol) was added in small portions over 1 h. The product solution was stirred for 5 h at 70 °C and for 12 h at room temperature; the emerging purple precipitate was collected by filtration and washed with ethanol and diethyl ether.

Compound a was isolated after recrystallization of the crude product from ethanol 0.1 M $HClO_4$ (5:1). The resulting purple crystals were collected and washed with ethanol ether and air-dried (555 mg, 6%). Anal. Calcd for $C_{20}H_{30}Cl_2CuN_6O_8$: C, 38.94; H, 4.90; N, 13.62; Cl, 11.49. Found: C, 38.97; H, 4.90; N, 13.54; Cl, 11.44. Electronic

(66) Gans, P.; Sabatinil, A.; Vacca, A. *J. Chem. Soc., Dalton Trans.* **1985**, 1195.
(67) Motekaitis, R. J.; Martell, A. E. *Can. J. Chem.* **1982**, *60*, 2403.

spectrum (H_2O) [λ_{max}, nm (ϵ, $dm^3\ mol^{-1}\ cm^{-1}$]: 506 (63). Infrared spectrum (KBr) (cm^{-1}): 3442 (br, m, H_2O); 3233 (m, NH); 1595, 1481 (m, py); 1107, 621 (br, s, ClO_4^-). Several additional crops were obtained from the filtrate; the last one produced X-ray-quality crystals of the syn isomer b.

For the isolation of compound c the crude product was dissolved in a small amount of 0.5 M HCl, diluted to 2 L with water, and sorbed onto a column of Dowex 50Wx2 cation-exchange resin (100 × 5 cm, H^+ form). With 2 M HCl (approximately 1.5 L) a first violet band was eluted and then a second one with 3 M HCl (approximately 1 L) and a very small third one with 4 M HCl (approximately 1.5 L). Every fraction was evaporated to dryness and recrystallized from ethanol/0.1 M $HClO_4$ (10:1). From fraction one and two purple and violet crystals were obtained (ratio 5:1). Recrystallization of the third fraction yielded violet crystals. Electronic spectrum (H_2O) [λ_{max}, nm (ϵ, $dm^3\ mol^{-1}\ cm^{-1}$]: 516 (192), pH 7; 525, pH 1.

***anti*-6,13-Bis(2-pyridinyl)-1,4,8,11-tetraazacyclotetradecane Hexahydrochloride.** The crude reaction mixture of copper complexes (830 mg) was dissolved in 0.5 M HCl (30 mL), diluted to 2 L with distilled water, and sorbed onto a column of sephadex-SP C 25 cation exchange resin (Na^+ form; 90 × 5 cm). With 0.2 M NaCl a first violet fraction (λ_{max} = 523 nm), with 0.3−0.4 M NaCl a broad second fraction (λ_{max} = 525 nm), and with 0.4−0.5 M NaCl a small third fraction (λ_{max} = 527 nm) were eluted. The three fractions were concentrated each to approximately 50 mL on a rotary evaporater, NaCl was removed by filtration, and the fractions were reduced separately; they were added dropwise (vigorous stirring) to 0.5 g of Zn dust, suspended in 2 M HCl. Over 1 h, additional Zn dust (1.5 g) was added in small portions, so that no residual purple color remained when the next aliquot was added. The colorless mixture was then filtered to remove solids, the pH was adjusted to 2, and the solution was diluted to 1 L. This was sorbed onto a column of Dowex 50Wx2 cation exchange resin (50 × 5 cm H^+ form). The column was washed with 1 M HCl to remove $Zn(aq)_2^+$ (identified by neutralizing aliquotes of the eluate to afford a precipitate of $Zn(OH)_2$). The protonated ligand eluted slowly with 3 M HCl. The eluent was evaporated to dryness washed several times with ethanol and air-dried. Yield: fraction 1, 155 mg (0.271 mmol); fraction 2, 240 mg (0.418 mmol); fraction 3, 136 mg (0.238 mmol). ^1H and ^{13}C NMR show that only fraction 3 is the pure anti isomer. Recrystallization from ethanol/H_2O (1:1) produced, after addition of $NaClO_4$, colorless crystals of (a-pypymacH4)$(ClO_4)_4$·$2H_2O$, suitable for an X-ray analysis. The analytical data are for a-pypymac·6HCl·H_2O. Anal. Calcd for $C_{20}H_{36}Cl_6N_6$·H_2O: C, 40.63; H, 6.48; N, 14.21; Cl, 35.96. Found: C, 40.57; H, 6.59; N, 14.22; Cl, 35.15. ^1H NMR (D_2O/CD_3CN): δ 2.93, 3.15 (AA′XX′ system, 2 × 4H, NHC$\mathbf{H}_A$$\mathbf{H}_XC\mathbf{H}_{A'}$ $H_{X'}$NH, $^2J_{AX}$ = −13.4 Hz, $^3J_{AA'}$ = 11.8 Hz, $^3J_{AX'}$ = 3 Hz, $^3J_{XX'}$ = 3.7 Hz), 3.38−3.44 (mult, 8 H, $NHCH_2CH$), 3.67−3.73 (mult, 2 H, $NHCH_2CH$); 7.91−7.95 (mult, 4 H, meta-C$\mathbf{H}_{arom}$), 8.53 (dt, 2 H, para-CH_{arom}) ^3J = 8.0 Hz, ^4J = 1.5 Hz), 8.66 (dd, 2 H, ortho-CH_{arom}, ^3J = 5.9 Hz, ^5J = 1.0 Hz). ^{13}C NMR (D_2O/CD_3CN): δ 40.64 (CH), 47.55 ($CH_{2,cap.}$), 52.89 ($CH_{2,en}$), 126.82, 127.51, 142.84, 148.84, 152.27 (C_{arom}).

[*syn*-6,13-Bis(2-pyridyl)-1,4,8,11-tetraazacyclotetradecane]cobalt(III) Chloride Pentahydrate. The isomeric mixture of [Cu(s/a-pypymac)$(ClO_4)_2$] (414 mg, 0.672 mmol) was dissolved in dry EtOH (40 mL) under Ar. The solution was stirred at 80 °C for 1 h. After cooling of the solution to approximately 50 °C, two spatulas of Raney alloy W2 and NH_2-NH_2·H_2O (1.5 mL) were added slowly. After 2 h of stirring the solution became almost colorless and no further N_2 was observed. After being stirred for 30 min at 50 °C, the solution was refluxed for 30 min to destroy excess NH_2-NH_2·H_2O. The catalyst was filtered at room temperature, and $Co(BF_4)_2$·$6H_2O$ (225 mg, 0.672 mmol) and charcoal were added. The red solution was aerated for 2 h and stirred at room temperature for additional 12 h. After filtration the solution was diluted to 1 L and sorbed onto a Sephadex SP C 25 cation-exchange resin (Na^+ form, 3 × 30 cm) eluted. A small red fraction of uncomplexed Co^{2+} is eluted with 0.2 M $NaBF_4$, followed by the eluation with 0.3 M $NaBF_4$ of two orange fractions. To eliminate $NaBF_4$ these fractions each were sorbed onto a Dowex 50 Wx2 cation-exchange resin (3 × 7 cm) and washed with 2 L of distilled water and 1 L of 0.5 M HCl. The cobalt(III) complexes were eluted with 2 M HCl, and the solutions were evaporated to dryness. The orange complexes were washed with ethanol and diethyl ether. The first fraction (171 mg; 47%) was identified as the anti isomer (see below). The second fraction was pure syn isomer (40 mg; 11%). Recrystallization from ethanol/H_2O (1:1) yielded orange crystals suitable for an X-ray analysis. Anal. Calcd for $C_{20}H_{30}Cl_3CoN_6$·$3.5H_2O$: C, 41.21; H, 6.40; N, 14.42. Found: C, 41.00; H, 5.92; N, 14.30. Electronic spectrum (H_2O) [λ_{max}, nm (ϵ, $dm^3\ mol^{-1}\ cm^{-1}$]: 466 (45), 342 (sh). Reduction portential (100 mV/s; V vs NHE): −0.35, Co(III/II). Infrared spectrum (KBr) (cm^{-1}): 3441 (br, s, H_2O); 3068 (s, NH); 2857 (s, CH); 1610, 1448 (Py). ^1H NMR (D_2O/TSP): δ 1.78 (dt; 2H; ^2J = 26.5 Hz, ^3J = 3.8 Hz; NC$\mathbf{H}_E$HCH$_2$N); 2.83 (dd; 2H; ^2J = −13.8 Hz; ^3J = 2.8 Hz; NC$\mathbf{H}_G$H$_I$CH); 2.94−3.07 (m; $NCH_A\mathbf{H}_BCH$; NC$\mathbf{H}_C$H$_D$CH$_2$N; $NCH_2CH_D\mathbf{H}_F$N); 3.28 (dd, 2H, ^2J = −13.0 Hz, ^3J = 3.7 Hz; $NCH_2C\mathbf{H}_D$H$_F$N); 3.49 (d, ^2J = −13.7 H$_2$; NC$\mathbf{H}_A$H$_B$CH); 3.64 (d, ^2J = −13.6 Hz, NCH$_G$$\mathbf{H}_I$CH); 4.79 (brs, C$\mathbf{H}_K$-Pyr); 7.64 (t, ^3J = 13.6 Hz, ^4J = 1.2 Hz meta to N); 7.91 (d, ^3J = 7.1 Hz meta to N); 8.01 (d, 2H, ^3J = 5.8 Hz ortho to N); 8.29 (t, 2H, ^3J = 14.8 Hz, ^4J = 0.8 Hz, para to N).

[*anti*-6,13-Bis(2-pyridyl)-1,4,18,11-tetraazacyclotetradecane]cobalt(III) Chloride. The stirred solution of the isomeric mixture of *syn*-/*anti*-6,13-bis(2-pyridyl)-1,4,8,11-tetraazacyclotetradecane) hexahydrochloride in 20 mL of distilled water was adjusted to pH = 8, and 322 mg (0.945 mmol) of $Co(BF_4)_2$·$6H_2O$ and 500 mg of charcoal were added. The solution was aerated for 6 h. After being stirred for 12 h at room temperature, the solution was filtered, diluted to 1 L, and sorbed onto a column of Sephadex-SP C 25 cation-exchange resin (Na^+ form, 60 × 5 cm). With 0.2 M $NaBF_4$ the excess of $Co(BF_4)_2$ was eluted first as a red fraction. With 0.3−0.4 M $NaBF_4$ a major yellow and with 0.4−0.5 M $NaBF_4$ a minor orange fraction were eluted. To purify the products, each fraction was sorbed onto a Dowex 50 Wx2 cation-exchange column (10 × 3 cm). After being washed with 2 L of H_2O and 1.5 L of 0.5 M HCl, the fractions were eluted with 2 M HCl and evaporated to dryness. NMR spectra show that the orange fraction consists of a crude mixture, which probably includes $[Co(s\text{-}pypymac)]^{3+}$ and various aqua- and chlorocobalt(III) complexes; NMR spectra, elemental analyses, and UV−vis and IR spectra of the yellow fraction indicate that this is pure $[Co(a\text{-}pypymac)]Cl_3$·$H_2O$ (207 mg, 42%). Recrystallization from 0.1 M $HClO_4$ (1:3) yielded yellow-orange crystals suitable for an X-ray analysis. The analytical data are for the chloride salt. Anal. Calcd for $C_{20}H_{30}Cl_3CoN_6$·H_2O: C, 44.67; H, 6.00; N, 15.63; Cl, 19.78. Found: C, 44.21; H, 6.00; N, 15.36; Cl, 19.17. Electronic spectrum (H_2O) [λ_{max}, nm (ϵ, $dm^3\ mol^{-1}\ cm^{-1}$]: 464 (75), 347 (sh). Reduction potential (100 mV/s; V vs NHE]: −0.31, Co(III/II). Infrared spectrum (KBr) (cm^{-1}): 3260 (s, NH); 2864 (s, CH); 1613, 1450 (Py). ^1H NMR (D_2O/TSP): δ 1.72, 2.84 (AA′XX′ system, 2 × 4 H, $^2J_{DE}$ = −13.0 Hz, $^3J_{DD''}$ = 13.9 Hz, $^3J_{DE'}$ = 3.9 Hz; $^3J_{EE'}$ = 1.0 Hz; NHC$\mathbf{H}_D$$\mathbf{H}_EC\mathbf{H}_{D''}$$\mathbf{H}_{E''}$NH); 2.78, 3.79 (AB part of the ABX system, 2 × 4 H, $^2J_{AB}$ = −13.5 Hz, $^3J_{AC}$ = 3.8 Hz, $^3J_{BC}$ = 1.7 Hz, NHC$\mathbf{H}_A$$\mathbf{H}_B$-CH); 4.19 (m, 2H, $NHCH_A\mathbf{H}_BC\mathbf{H}_C$); 7.93 (dd, 2H, $^4J_{HH}$ =1.2 Hz, $^3J_{HH}$ = 7.8 Hz, $C_qC\mathbf{H}$); 7.98 (dt, 2H, $^4J_{HH}$ = 1.5 Hz, $^3J_{HH}$ = 10.2 Hz, C$\mathbf{H}$ meta to N); 8.36 (dt, 2H, $^4J_{HH}$ = 1.3 Hz, $^3J_{HH}$ = 7.7 Hz, C$\mathbf{H}$ para to N); 8.96 (d, 2H, $^3J_{HH}$ = 5.5 Hz, C$\mathbf{H}$ ortho to N). ^{13}C NMR (D_2O/TSP): δ 48.83 (**CH**); 52.01, 58.19 ($\mathbf{C}H_2$); 130.83, 146.39, 155.77 ($\mathbf{C}H_{arom}$); 161.88 ($\mathbf{C}_{arom}$, ^3J = 5.8 ortho to N); 8.29 (t, ^3J = 14.8 Hz, ^4J = 0.8 Hz para to N). ^{13}C NMR (D_2O/TSP): δ 49.10 (**C**H); 50.58, 51.67 ($\mathbf{C}H_{2,cap}$); 57.35, 58.94 ($\mathbf{C}H_{2,en}$); 129.60, 130.68, 146.18, 157.30 ($\mathbf{C}H_{arom}$); 163.532 ($\mathbf{C}_{arom}$).

[*anti*-6,13-Bis(2-pyridyl)-1,4,8,11-tetraazacyclotetradecane]nickel(II) Perchlorate. A solution of 157 mg (0.274 mmol) of *anti*-6,13-bis(2-pyridyl)-1,4,8,11-tetraazacyclotetradecane hydrochloride in 10 mL of distilled water was adjusted to pH = 9. A 100 mg (0.274 mmol) amount of $Ni(ClO_4)_2$·$6H_2O$ dissolved in 3 mL of water was added dropwise. The mixture was allowed to stand at room temperature for several days, and the bright pink crystals, suitable for an X-ray analysis, were collected and dried under vacuum (130 mg, 77%). Anal. Calcd for $C_{20}H_{30}Cl_2N_6NiO_8$: C, 39.24; H, 4.94; N, 13.73; Cl, 11.58. Found: C, 39.20; H, 4.87; N, 13.71; Cl, 11.54. Electronic spectrum (CH_3CN) [λ_{max}, nm (ϵ, $dm^3\ mol^{-1}\ cm^{-1}$]: 766 (9), 484 (12), 321 (293). Reduction potential (100 mV/s, acetonitrile, Ag/$AgNO_3$) [V vs ferrocenium/ferrocene]: 0.641 (quasi reversible). Infrared spectrum (KBr) (cm^{-1}):

3290 (s, NH); 2874 (m, CH); 1605, 1486 (s, pyridine); 1090, 624 (br, s, ClO_4^-).

[*anti*-6,13-Bis(2-pyridyl)-1,4,8,11-tetraazacyclotetradecane]zinc-(II) Hexafluorophosphate. A 165 mg amount of *anti*-6,13-bis(2-pyridyl)-1,4,8,11-tetraazacyclotetradecane hydrochloride was dissolved in water (500 mL) and sorbed onto an Amberlite IRA-416 anion-exchange resin. The free ligand was eluted with 2 L of distilled water and evaporated to dryness. The yield was assumed to be quantitative. The free amine was dissolved in a mixture of methanol/water (1:1), and a solution of 111 mg (0.466 mmol) of $Zn(BF_4)_2 \cdot 6H_2O$ in water (5 mL) was added dropwise. After the solution was stirring for 12 h at room temperature, 152 mg (0.932 mmol) of NH_4PF_6 was added. The colorless product was filtered out, washed with H_2O, and dried over phosphorus pentoxide (175 mg, 53%). The product was recrystallized from a mixture of CH_3CN/H_2O (3:1) and left standing. The colorless crystals, suitable for X-ray analysis, were collected and washed with water and air-dried. Anal. Calcd for $C_{20}H_{30}F_{12}N_6P_2Zn$: C, 33.84; H, 4.26; N, 11.84; P, 8.73. Found: C, 33.86; H, 4.47; N, 11.81; P, 8.59. Infrared spectrum (KBr) (cm^{-1}): 3328 (m, NH) 1605, 1449 (w, pyridine); 636 (s), 557 (m, PF_6). ^1H NMR (CD_3NO_2): aliphatic protons, δ 2.0−2.18 (m), 3.08−3.21 (m), 4.02−4.10 (m); aromatic protons, δ 7.56 (d, $^3J = 7.18$ Hz, C_qCH), 7.64 (dt, $^4J = 1.74$ Hz, $^3J = 6.18$ Hz, C**H** meta to N_{Py}); 8.08 (dt, $^4J = 1.55$ Hz, $^3J = 7.75$ Hz, C**H** para to N_{Py}); 8.71 (d, $^3J = 4.9$ Hz, C**H** ortho to N_{Py}). ^{13}C NMR (CD_3NO_2): δ 44.53, 51.40, 54.38 (**C**H, **C**H_2); 125.38, 125.97, 141.63, 150.43, 162.54 (**C**$_{Py}$).

Acknowledgment. Generous financial support by the German Science Foundation (DFG) is gratefully acknowledged.

Supporting Information Available: ORTEP plots of the four structurally characterized intermediates and/or side products of the template reaction (ligands L^1−L^4), NMR analysis spectra of the metal-free ligand and the cobalt(III) complexes, preliminary titration plots of a-pypymac, and tables of crystallographic data. This material is available free of charge via the Internet at http://pubs.acs.org.

IC000696X